Protein Structure and Folding:

Structural Evidence That Colicin A Protein Binds to a Novel Binding Site of TolA Protein in *Escherichia coli* Periplasm

Chan Li, Ying Zhang, Mireille Vankemmelbeke, Oliver Hecht, Fadilah Sfouq Aleanizy, Colin Macdonald, Geoffrey R. Moore, Richard James and Christopher N. Penfold

J. Biol. Chem. 2012, 287:19048-19057.
doi: 10.1074/jbc.M112.342246 originally published online April 9, 2012

THE JOURNAL OF BIOLOGICAL CHEMISTRY VOL. 287, NO. 23, pp. 19048–19057, June 1, 2012

Structural Evidence That Colicin A Protein Binds to a Novel Binding Site of TolA Protein in *Escherichia coli* Periplasm*[S]

Received for publication, January 18, 2012, and in revised form, March 22, 2012 Published, JBC Papers in Press, April 9, 2012, DOI 10.1074/jbc.M112.342246

Chan Li[‡1,2], Ying Zhang[‡1], Mireille Vankemmelbeke[‡], Oliver Hecht[§], Fadilah Sfouq Aleanizy[‡], Colin Macdonald[§], Geoffrey R. Moore[§], Richard James[‡], and Christopher N. Penfold[‡3]

From the [‡]School of Molecular Medical Sciences, Centre for Biomolecular Sciences, University of Nottingham, University Park, Nottingham NG7 2RD and the [§]Centre for Molecular and Structural Biochemistry, School of Chemical Sciences, University of East Anglia, Norwich NR4 7TJ, United Kingdom

Background: Colicins interact with Tol proteins in the periplasm to facilitate their killing of *E. coli* cells.
Results: The N terminus of colicin A interacts with the C terminus of TolA through β-strand addition.
Conclusion: Colicin A interacts with TolA at a novel binding site to promote cell killing.
Significance: TolA is integral to cell entry of colicin A, providing information to refine current models of colicin translocation.

The Tol assembly of proteins is an interacting network of proteins located in the *Escherichia coli* cell envelope that transduces energy and contributes to cell integrity. TolA is central to this network linking the inner and outer membranes by interactions with TolQ, TolR, TolB, and Pal. Group A colicins, such as ColA, parasitize the Tol network through interactions with TolA and/or TolB to facilitate translocation through the cell envelope to reach their cytotoxic site of action. We have determined the first structure of the C-terminal domain of TolA (TolAIII) bound to an N-terminal ColA polypeptide ($TA_{53–107}$). The interface region of the $TA_{53–107}$-TolAIII complex consists of polar contacts linking residues Arg-92 to Arg-96 of ColA with residues Leu-375–Pro-380 of TolA, which constitutes a β-strand addition commonly seen in more promiscuous protein-protein contacts. The interface region also includes three cation-π interactions (Tyr-58–Lys-368, Tyr-90–Lys-379, Phe-94–Lys-396), which have not been observed in any other colicin-Tol protein complex. Mutagenesis of the interface residues of ColA or TolA revealed that the effect on the interaction was cumulative; single mutations of either partner had no effect on ColA activity, whereas mutations of three or more residues significantly reduced ColA activity. Mutagenesis of the aromatic ring component of the cation-π interacting residues showed Tyr-58 of ColA to be essential for the stability of complex formation. $TA_{53–107}$ binds on the opposite side of TolAIII to that used by g3p, ColN, or TolB, illustrating the flexible nature of TolA as a periplasmic hub protein.

The Tol-Pal[4] network of proteins in the periplasm of Gram-negative bacteria is intriguing as conservation of the sequence of genes of the *tol-pal* operon across a variety of bacterial orders (1) suggests important functional significance of the Tol proteins. Although their normal cellular function in *Escherichia coli* is still uncertain (1), they appear to play a role in maintaining the integrity of the cell envelope, transducing energy from the cytoplasmic membrane, and may form a dynamic subcomplex at constriction sites to promote the energy-dependent septal wall formation across invaginating peptidoglycan and inner membrane layers during cell division (2–4). The Tol-Pal system consists of five proteins, TolA, TolB, TolQ, TolR, and peptidoglycan-associated lipoprotein (Pal). TolA is a 44-kDa periplasmic protein organized into three domains separated by clusters of glycine residues. It is anchored to the cytoplasmic membrane via a single transmembrane region (TolAI)[5] that is important for interactions with the TolQ and TolR proteins in the membrane (5), spans the periplasm via its extended central domain (TolAII), and binds to both TolB (6, 7) and Pal (8) via its C-terminal domain (TolAIII). TolQ and TolR are transmembrane proteins that are involved in the proton motif force-dependent activation of TolA (2), which shuttles energy from the inner to outer membrane through its association with Pal anchored to the outer membrane (9, 10). TolB is a periplasmic protein that is associated with the outer membrane via an interaction of its C-terminal β-propeller domain with Pal (11) and with TolA via its N-terminal domain (6).

ColA is a pore-forming colicin that forms pores in the cytoplasmic membrane of *E. coli* cells (12). The N-terminal translocation domain of ColA contains a binding region from residues 52–97 that interacts directly with TolAIII (13, 14). A TolA binding motif with a conserved tyrosine residue has been identified at two locations (^{57}SYNT^{60} and ^{89}PYGR^{92}) within the

* This work was supported by the Biotechnology and Biological Sciences Research Council, the Wolfson Foundation, and The Wellcome Trust.
⌘ *Author's Choice*—Final version full access.
[S] This article contains supplemental Figs. S1–S7 and Table S1.
The atomic coordinates and structure factors (codes 3QDP and 3QDR) have been deposited in the Protein Data Bank, Research Collaboratory for Structural Bioinformatics, Rutgers University, New Brunswick, NJ (http://www.rcsb.org/).

[1] Both authors contributed equally to this work.
[2] Present address: School of Pharmacy, Centre for Biomolecular Sciences, University of Nottingham, Nottingham NG7 2RD, United Kingdom.
[3] To whom correspondence should be addressed. Tel.: 44-1158467957; Fax: 44-115 8467951; E-mail: chris.penfold@nottingham.ac.uk.

[4] The abbreviations used are: Pal, peptidoglycan-associated lipoprotein; ColA, colicin A; g3p, gene 3 protein of bacteriophage fd; r.m.s., root mean square; r.m.s.d., root mean square distance; HSQC, heteronuclear single quantum correlation.
[5] The following designations are used for TolA domains throughout this manuscript: TolAI, domain one of TolA consisting of N-terminal residues, 1–47; TolAII, domain two consisting of residues 48–313; TolAIII, domain three of TolA consisting of C-terminal residues 314–421.

TolA box region of ColA with good homology to a TolA binding motif in the C-terminal domain of Pal (15). TolA is also required for the entry of ColN (16) and for the import of filamentous bacteriophage DNA into *E. coli* cells (17) through an interaction with the gene 3 protein of bacteriophage fd (g3p), which is a minor coat protein located at the end of the phage capsid (18).

Protein-protein interactions are crucial for the translocation of colicin domains into target cells, but the temporal and spatial relationships between Tol proteins and colicin domains are only just starting to be elucidated (19, 20). X-ray structures of members of the Tol-Pal assembly in complex with partner proteins have provided valuable information in deciphering the sequence of events that occur when group A colicins parasitize a sensitive cell (21–24). A solution structure of TolAIII (Protein Data Bank (PDB) ID: 1S62) (25) and an x-ray structure of a fusion formed from TolAIII and g3p (PDB ID: 1Tol) (26) have been reported, but despite its pivotal role in the Tol assembly of proteins and availability for binding to foreign polypeptides, a structure of TolAIII in complex with other Tol proteins or with colicin domains has not previously been reported. The present work aims to address the role of TolAIII in the uptake of ColA through determination of the x-ray crystal structures of *E. coli* TolAIII on its own and in complex with the TolA binding region of ColA.

EXPERIMENTAL PROCEDURES

Overexpression and Purification—E. coli B834(DE3) was used as an expression host for plasmids pYZ48 (residues 302–421 of TolA (TolAIII) cloned into pET21a via NdeI/XhoI restriction sites with an in-frame N-terminal His_6 tag) or pYZ69 (27) to purify TolAIII and TA_{1-107} [6] containing a thrombin recognition site after residue 52, respectively. An overnight culture of 10 ml of Luria Bertani medium (LB) was used to inoculate 0.5 liter of 2×YT broth supplemented with ampicillin (Melford Laboratories) to a final concentration of 100 μg/ml. Cultures were shaken in 2-liter baffled flasks at 180 rpm at 37 °C until they reached an A_{600} of 0.6–0.8; protein expression was induced for a period of 4 h after adding isopropyl-β-D-thiogalactopyranoside to a final concentration of 1 mM. For selenomethionine-labeled protein expression, *E. coli* 834 (DE3) harboring pYZ48 or pYZ69 was used as the expression host. The pellet from a 5-ml overnight culture grown in LB supplemented with ampicillin and chloramphenicol (34 μg/ml) was resuspended in 5 ml of sterile 0.9% NaCl and incubated in a shaker at 37 °C for 30 min, and the cells were spun down and washed again with 5 ml of sterile 0.9% NaCl before the pellet was transferred into 100 ml of Selenomethionine medium complete (Molecular Dimensions Ltd.) containing L-methionine and grown overnight at 37 °C. The overnight culture was washed twice in 0.9% sterile NaCl as described previously, and the pellet was transferred into 500 ml of selenomethionine medium complete containing L-selenomethionine before protein induction was carried out for 4 h at 37 °C with 1 mM isopropyl-β-D-thiogalactopyranoside when the cell A_{600} reached 0.6–0.8.

Once resuspended in a buffer containing 50 mM Tris-HCl, pH 8.0, 300 mM NaCl, 10 mM imidazole (lysis buffer), the cell pellets were lysed by sonication, and the lysate was centrifuged at 27,000 × *g* for 30 min. The supernatant was filtered into nickel-agarose beads (nickel-nitrilotriacetic acid, Qiagen), which were previously equilibrated with lysis buffer and gently mixed by circular rotation in a cold room for 1 h. The beads were washed with 50 mM Tris-HCl, pH 8.0, 300 mM NaCl, 10–30 mM imidazole (wash buffer), and finally, the proteins were eluted with 50 mM Tris-HCl, pH 8.0, 300 mM NaCl, 250 mM imidazole (elution buffer).

A region of TA_{1-107} containing a TolA binding site (TA_{53-107}) was separated from the TolB box by digestion of TA_{1-107} with thrombin at a thrombin recognition site engineered into TA_{1-107} after residue 52. The protein concentration was adjusted to 1 mg/ml in 20 mM Tris, pH 8.0, 100 mM NaCl containing 5 units/mg of thrombin (Haematologic Technologies Inc., Essex Junction, VT), and the mixture was left on a circulating platform rotor at room temperature overnight. The thrombin was then removed using ρ-aminobenzamidine-agarose beads (Sigma) according to the manufacturer's instructions, and TA_{53-107} was purified using metal chelate chromatography and nickel-agarose beads in His tag lysis buffer as described previously (27). TA_{53-107} was finally loaded to a Superdex 75 gel filtration column (GE Healthcare) to remove any undigested TA_{1-107}. The purity of protein samples was checked by running 15–17% SDS-PAGE gels. Pure fractions of TA_{53-107} were combined, concentrated using 5-kDa molecular mass cut off concentrators (Vivascience), and dialyzed to 20 mM Tris, pH 8.0, 100 mM NaCl. Protein concentration was determined by using absorption at 280 nm and extinction coefficients of 15,470, 8480, and 6085 $M^{-1}cm^{-1}$ for TA_{1-107} with a thrombin cleavage site after residue 52, TA_{53-107}, and TolAIII, respectively.

NMR Spectroscopy—Isotopically labeled TolAIII comprising amino acids 302–421 of the *E. coli* TolA protein (Swiss-Prot accession number P19934) and TA_{1-52} and TA_{53-107} containing the TolB box and TolA binding region of ColA, respectively, were prepared as described previously (27). The B^{1-13} peptide representing the N-terminal sequence of TolB lacking its signal peptide and comprising residues 21–33 of TolB (AEVRIVIDSGVDS) was purchased from United Peptide Corp. at a purity of 95%. NMR spectra were acquired at the indicated temperatures using a Bruker Avance III 800-MHz spectrometer equipped with a triple resonance probe and pulse sequences incorporated into the Bruker Topspin 2.1 software. Resonance assignments of $^{13}C/^{15}N$-labeled TA_{53-107} in complex with unlabeled TolAIII (1.2 mM) were obtained from ^{1}H-^{15}N HSQC, CBCA(CO)NH, HNCACB, and HNCA spectra at 27 °C. NMR spectra were processed using NMRPipe (28) and analyzed in NMRView and CCPN-Analysis as described previously (29).

Formation and Methylation of TA_{53-107}-TolAIII Complex—TA_{53-107} and TolAIII in 20 mM Tris, pH 8.0, and 100 mM NaCl were mixed in a 1.1:1 molar ratio and incubated at 4 °C overnight. The mixed sample was loaded onto a Superdex 75 col-

[6] The following designations are used for residues throughout this manuscript: TA_{53-107}, residues 53–107 of the translocation domain of colicin A; TA_{1-107}, residues 1–107 of the translocation domain of colicin A; TA_{1-52}, residues 1–52 of the translocation domain of colicin A.

umn equilibrated with 20 mM Tris, pH 8.0, 100 mM NaCl and run at a flow rate of 1 ml/min on an FPLC system (ÄKTA). The elution fractions were checked by running on 17% SDS-PAGE gels. The methylation of the TolAIII-$TA_{53–107}$ complex was carried out using a published protocol (30, 31). Briefly, both $TA_{53–107}$ and TolAIII were exchanged into 50 mM Hepes, pH 7.5, 100 mM NaCl and were mixed in a 1.1:1 molar ratio. Then the complex was adjusted to 1 mg/ml or 0.5 mg/ml for methylation of the selenomethionine-labeled complex. Methylation was carried out by adding borane dimethylamine complex (Sigma), which is a reducing agent, followed by formaldehyde (Sigma) before an overnight incubation at 4 °C (30, 31). The reaction was quenched by adding Tris buffer, pH 8, to 20 mM, and then the product was concentrated and buffer-exchanged into 20 mM Tris, pH 8, 100 mM NaCl for gel filtration to remove the small reactants and excess $TA_{53–107}$.

Crystallization, X-ray Diffraction, and Model Refinement—The methylated $TA_{53–107}$-TolAIII complex was crystallized by using the sitting-drop vapor diffusion method at 20 °C with 2 μl of the complex at 35 mg/ml in 20 mM Tris-HCl, pH 8.0, 100 mM NaCl mixed in equal volumes with the reservoir solution containing 0.2 M K_2HPO_4, 2.2 M ammonium sulfate. The complex crystals grew after 3–4 weeks. Before being frozen in a nitrogen stream, crystals were soaked in 0.2 M KH_2PO_4, 2.26 M ammonium sulfate, and 1.1 M disodium malonate for cryoprotection. Diffraction data sets were collected at the European Synchrotron Radiation Facility (ESRF), Grenoble, France, using a MAR 225 detector at a microfocus beamline of ID23-2 ($\lambda = 0.8726$ Å) for native crystals and an ADSC Quantum Q315r detector at a beamline of ID14-4 ($\lambda = 0.9795$ Å) for selenomethionine-labeled crystals. A wavelength of 0.9795 Å was used for collecting the single anomalous dispersion data sets for selenomethionine-labeled crystals. After failure to get the phase from molecular replacement using the available TolAIII structures PDB ID 1Tol (26) and PDB ID 1S62 (25) as search models, selenomethionine-labeled crystals of this complex were used to obtain the phase.

All data were processed with XDS (32), converted from XDS format to mtz format with Pointless (33), and scaled in SCALA (34) of the CCP4 suite (35). The initial phase was determined by using Phaser-EP (36) with the coordinates of four anomalous atoms found by Solve (37). The phase was improved by running the Density Modification (DM) program (38) and extended from 2.8 Å of selenomethionine crystals to 2.65 Å of native crystals using Cad and Scaleit of the CCP4 suite. The initial model was built by using Buccaneer (39) with 100 cycles and COOT (40), and then the model was used as a search model for molecular replacement through the use of Phaser (36) against the native data, rebuilt in COOT, and refined using restrained and TLS refinement in REFMAC5 (41). The optimal number of TLS groups was determined using the TLSMD server (42). The final model has excellent geometry and no Ramachandran outliers. The data processing, phasing, and model refinement statistics are summarized in Table 1. Surface area accessibility calculations and cation-π interaction identifications were carried out using the programs AREAIMOL (43) and CaPTURE (44), respectively. All structural figures were prepared using PyMOL (67).

Colicin Activity Assay—Spot test assays of biological activity of ColA and ColA mutants were conducted as described previously (45).

PCR Mutagenesis—Point mutations of the ColA gene were generated using the QuikChange II site-directed mutagenesis kit (Stratagene) according to the manufacturer's instructions. All constructs were verified by DNA sequencing (Source BioScience, Nottingham, UK).

Surface Plasmon Resonance—Surface plasmon resonance assays were conducted as described previously (24). TolAIII was immobilized to the matrix of a newly docked CM5 sensor chip, pre-equilibrated in HBS-EP running buffer (10 mM Hepes, 150 mM NaCl, 3 mM EDTA, 0.005% Tween) (BIAcore AB) via amine coupling to a level of immobilization of 200 response units. Two-minute injections of 10 μM of the ColA and ColA mutant proteins were performed across the immobilized TolAIII on the CM5 chip at a flow rate of 30 μl/min. After each analyte injection, the sensor chip surface was regenerated using a 2-min pulse of 10 mM glycine, pH 1.8. Global analysis using BIAevaluation software 3.1 was used to align all the binding curves. To determine the binding affinity data, 2-min injections of a range of concentrations of $TA_{1–107}$ or $TA_{53–107}$ were performed using the same TolAIII chip. Global analysis using BIAevaluation software 3.1 was used to fit corrected surface plasmon resonance responses to the theoretical 1:1 Langmuir binding model.

RESULTS

Crystallization of $TA_{53–107}$-TolAIII Complex—Initially, we were unable to obtain crystals of TolAIII in complex with a polypeptide of ColA expressing residues 1–107 ($TA_{1–107}$). Disorder analysis of the sequence of $TA_{1–107}$, using the RONN program (46), showed that the N terminus of ColA containing the TolB box (residues 11–20) is disordered (47–49), whereas a region containing residues 52–97, predicted to contain the TolAIII binding region of ColA (50), was ordered (supplemental Fig. S1). The $TA_{53–107}$ polypeptide produced from the thrombin cleavage of $TA_{1–107}$ (see "Experimental Procedures") and lacking the TolB box was able to form a stable complex with TolAIII with a binding affinity of 1.34 ± 0.008 μM (data not shown). However, only tiny protein crystals grew from crystallization screens of the $TA_{53–107}$-TolAIII complex. High entropy residue analysis of TolAIII was performed by using a surface entropy reduction prediction server (51), which predicted five high entropy surface lysine residues in four clusters (supplemental Fig. S2). The reductive methylation of lysine residues has previously been reported to be a valuable rescue strategy for obtaining diffraction-quality crystals from proteins found previously difficult to crystallize (30). Crystals of a complex of selenomethionine-labeled TolAIII and $TA_{53–107}$ proteins, which was methylated before crystallization, appeared in the orthorhombic space group $P2_12_12$, with one TolAIII and one $TA_{53–107}$ polypeptide in the asymmetric unit and a solvent content of 58%.

Crystal Structure of $TA_{53–107}$-TolAIII Complex—The structure consists of residues 329–421 of TolAIII and residues 57–105 of $TA_{53–107}$, 26 water molecules, and one Tris ion (Fig. 1). Only Lys-351 of TolAIII was methylated in the $TA_{53–107}$-TolAIII complex. The structure was refined to a resolution of

2.65 Å with the R_{factor} and R_{free} being 24.4 and 27.3%, respectively (Table 1). The structure of TolAIII consists of three α-helices and three β-strands with a short helix between the first α-helix and the first β-strand. There are two small β-sheets in TA_{53-107} located in its C and N terminus, respectively, each composed of two β-strands connected by a hairpin. Thus the structure of TA_{53-107} is like a skipping rope with two small β-sheets at the C terminus and N terminus acting as the two handgrips of the rope. The N-terminal β-sheet forms four intramolecular hydrogen bonds, whereas the C-terminal β-sheet forms eight, all of them formed between the backbone atoms. The β-sheet at the C terminus of TA_{53-107} forms an intermolecular antiparallel β-sheet with the three β-strands of TolAIII. The remainder of TA_{53-107}, mainly between the two small β-sheets, forms a hairpin and loops. Therefore, the complex forms a five β-strand sheet, with the α-helices of TolAIII on one side and the N-terminal small β-sheet, together with the hairpin and loops of TolA box, on the other side of the five β-strand sheet of the complex (Fig. 1). There are no similar structures to that of TA_{53-107} available in the PDB database from search results using the Dali server.

Binding Interface between TA_{53-107} and TolAIII—The binding interface between TA_{53-107} and TolAIII buries a total surface area of 1303 Å with TolAIII and TA_{53-107} contributing 683 and 620 Å, respectively. The buried surface area is in the range of 1200–2000 Å that has been observed for most heterodimeric protein-protein complexes (52, 53). The calculated shape complementarity index, (S_c) (54) is 0.72, which is higher than that of high affinity protein-protein complexes such as the colicin E3 DNase-Im3 and colicin E9 DNase-Im9 complexes, indicating a high level of complementarity between TolAIII and TA_{53-107} in the complex. The interactions between TolAIII and TA_{53-107} encompass mainly electrostatic interactions and hydrophobic/apolar contacts. There are six direct hydrogen bonds between residues 92–96 of TA_{53-107} and residues 375–380 of TolAIII with the two protruding side chains Arg-92 and Arg-96 from

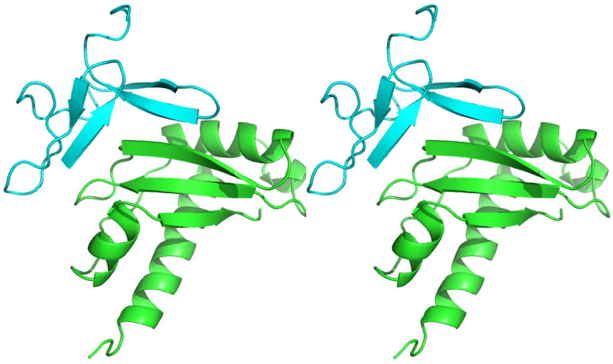

FIGURE 1. **Structure of TA_{53-107}-TolAIII complex.** A stereo image of the secondary structure of TA_{53-107} (*cyan*) in complex with TolAIII (*green*) displaying a classical β-sheet augmentation pattern of complex formation is shown.

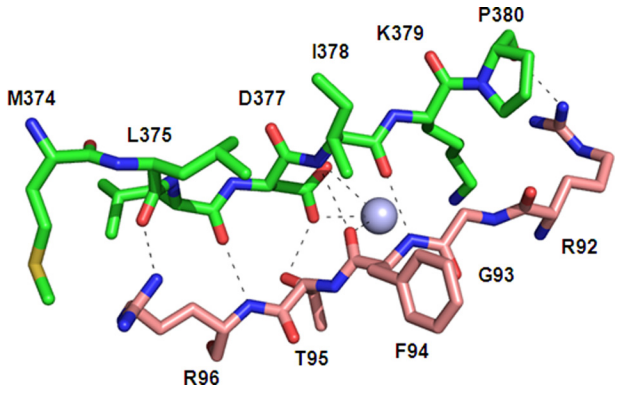

FIGURE 2. **Binding interface of TA_{53-107}-TolAIII complex.** A *ball and stick representation* of the interface between TA_{53-107} (*pink*) and TolAIII (*green*) is shown. Intermolecular hydrogen bonds either direct or mediated by a water molecule (*gray sphere*), between interacting residues are shown as *hyphenated lines*.

TABLE 1
Data collection and refinement statistics

	TolAIII	TA_{53-107}-TolAIII	
		Native	Se-Met
Data collection			
Space group	$P3_1\,2\,1$	$P2_1\,2_1\,2$	$P2_1\,2_1\,2$
Cell dimensions *a*, *b*, *c* (Å)	70.28, 70.28, 53.82	47.50, 119.62, 30.15	47.10,118.69, 29.85
Wavelength, Å	0.9792	0.8726	0.9795
Resolution range, Å	40.32–2.15 (2.27–2.15)	44.14–2.65 (2.79–2.65)	43.81–2.8 (2.95–2.8)
No. of unique reflections	8641 (1234)	5238 (757)	4356 (585)
Total no. of observations	84,194 (12,226)	18,767 (2757)	50,579 (3176)
Redundancy	9.7 (9.9)	3.6 (3.6)	11.6 (5.4)
Mean $I/\sigma(I)$	25.7 (5.0)	10.5 (3.8)	21.9 (5.7)
Completeness, %	100 (100)	97.4 (98.2)	97.3 (92.4)
R_{merge}, %	5.6 (43.3)	9.8 (34.4)	9.1 (30.4)
Anomalous completeness, %			96.5 (87.2)
Anomalous redundancy			6.5 (3.0)
Phasing statistics			
FOM[a] after PHASER			0.335
FOM after DM			0.528
FOM after Refmac5			0.797
Refinement statistics			
Resolution range, Å	60.87–2.15	59.81–2.65	
R_{work}/R_{free} %	19.2/22.5	24.4/27.3	
r.m.s. bond lengths, Å	0.0286	0.0137	
r.m.s. angles, °	2.371	1.867	
Average *B*-factor (protein, Å^2)	20.3	26.4	
No. of protein atoms	685	1059	
No. of water and ion atoms	52	34	
PDB accession code	3QDP	3QDR	

[a] FOM, figure of merit.

A

Clone	Interface residues				
	92	93	94	95	96
ColA	R	G	F	T	R
YZ106			A		
YZ107			A		A
YZ108	A				A
YZ109			A	A	A
YZ110	A	A	A	A	A

B

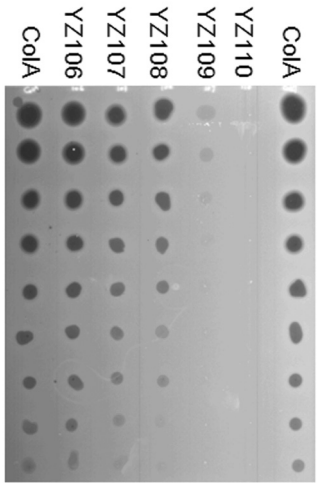

FIGURE 3. **Effects of TolA box mutations of ColA on activity of ColA are cumulative.** *A*, individual (pYZ106), double (pYZ107 and pYZ108), and multiple mutations of the TolA box of ColA (pYZ109 and pYZ110) were engineered using PCR mutagenesis, and the mutant polypeptides were purified and spotted onto a lawn of sensitive *E. coli* cells. *B*, zones of clearing indicative of cell killing were reduced in mutants containing successively more mutations and disappeared in all mutants containing three or more mutations.

TA_{53-107} forming hydrogen bonds with Pro-380 and Leu-375 of TolAIII (Fig. 2, supplemental Table S1). A water molecule mediates three hydrogen bonds between Phe-94 of TA_{53-107} and Asp-377 of TolAIII. The crystal structure of the TA_{53-107}-TolAIII complex indicates that the minimum size of the TolAIII binding region of ColA consists of residues 58–96, rather than the previously described residues 52–97 (50), which is still larger than the TolAIII binding region of colicin N (55).

Mutational Analysis of Interface Residues of TA_{53-107}-TolAIII Complex—Alanine-scanning mutagenesis of the five interface residues of ColA (Arg-92–Arg-96) that interact with TolAIII was performed, and the biological activity of the purified mutant proteins was assessed using a colicin plate assay (Fig. 3). Alanine mutations of any one of the five interface residues of ColA had little effect on biological activity, as can be seen for the F94A mutant of ColA in YZ106 (Fig. 3). The introduction of multiple alanine mutations of the interface residues revealed an additive effect that was observed as a reduction in biological activity of the mutant ColA. The presence of both the F94A and the R96A mutations (in YZ108) resulted in a further small reduction of biological activity when compared with YZ106 (Fig. 3). The further addition of a T95A mutation (in YZ109) resulted in a major reduction of biological activity. A complete loss of biological activity was seen with YZ110, in which all five of the interface residues were mutated to alanine.

In parallel, the contribution of the five residues of TolAIII to the binding interface of the TolAIII-TA_{53-107} complex was also

TABLE 2

Complementation of the TolA$^-$ mutant strain of *E. coli*, JC7782 with TolA and TolA containing various mutations expressed from the plasmid, pTol

Strain	TolAIII mutation	Complementation[a]
JC7782	TolA$^-$	>250 nM[b]
JC7782 (pTolA)	None	10 nM
JC7782 (pST1)	L375A	10 nM
JC7782 (pST2)	L376A	50 nM
JC7782 (pST3)	D377A	10 nM
JC7782 (pST4)	I378A	10 nM
JC7782 (pST5)	P380A	10 nM
JC7782 (pNP341)	L375A, D377A, P380A	50 nM
JC7782 (pNP342)	L375A, L376A, D377A, I378A, P380A	>250 nM[b]

[a] Complementation was assessed as the lowest concentration of colicin A that was able to produce a visible zone of inhibition on LB agar plates containing an overlay of the strain indicated in the table.

[b] Zones of inhibition were not seen in these strains at any concentration of ColA tested.

determined. Mutations were engineered into pTol, which expresses the TolA protein (56), and assayed for activity by complementation of the *tolA* mutant, *E. coli* JC7782. Individual alanine mutations of residues Leu-375, Leu-376, Asp-377, Ile-378, and Pro-380 of TolAIII were still able to complement the *tolA* mutant, resulting in the restoration of sensitivity to ColA, whereas a mutant containing alanine substitutions in all five residues that contribute to intermolecular contacts across the interface did not complement the *tolA* mutant (Table 2). Surprisingly, mutants of pTol containing alanine substitutions of Leu-376, Asp-377, and Pro-380 of TolAIII were still able to complement the *E. coli tolA* mutant, albeit at reduced levels (Table 2), despite the apparent loss of several important intermolecular polar contacts, particularly those contacts resulting from the side chain of Asp-377 (Fig. 2).

NMR and X-ray Structural Comparisons of TolAIII and TA_{53-107}-TolAIII—The x-ray structure of free TolAIII was obtained by chance in the process of the attempted crystallization of the complex formed between TolAIII and a peptide representing the N-terminal region of TolB lacking its signal peptide (referred to here as B^{1-13}). The complex was methylated, but the structure was solved with only TolAIII in the density without any extra density for B^{1-13}. Mass spectrometry analysis of the solubilized crystals proved that no peptide was present in the crystallized sample. Therefore, the structure we have obtained is that of TolAIII on its own.

The free TolAIII structure was refined to a resolution of 2.15 Å with R_{factor} and R_{free} being 19.2 and 22.5%, respectively. The first 32 residues have no corresponding electron density and are omitted in the model. Only three lysine residues (Lys-345, Lys-351, and Lys-413) were identified as being methylated, with lysines 345 and 413 being dimethylated and Lys-351 being monomethylated (supplemental Fig. S3). In addition, there are two nitrate ions and 43 water molecules in the model. The free x-ray structure has a marked similarity to the NMR structure of TolAIII (PDB ID: 1S62) (25) with three α-helices and three β-strands (supplemental Fig. S4). However, subtle differences exist that prevented our determination of the x-ray structure of free TolAIII by molecular replacement using PDB IDs 1S62 and 1Tol as search models, suggesting that there are some conformational differences between our free x-ray TolAIII structure and both the NMR solution structure of TolAIII and the x-ray

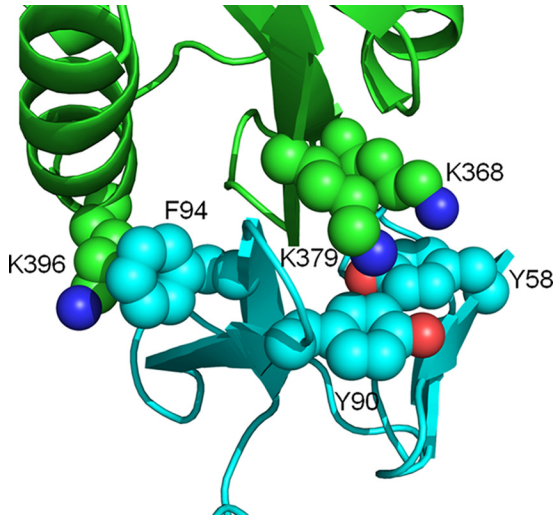

FIGURE 4. **Cation-π interactions across TA_{53-107}-TolAIII complex.** Electron-rich aromatic tyrosine (Tyr-58, Tyr-90) and phenylalanine (Phe-94) residues of the TolA box stack perpendicular to the positively charged side chains of lysine residues (Lys-368, Lys-379, Lys-396), forming cation-π interactions that strengthen and stabilize the interaction at the interface between the two polypeptides.

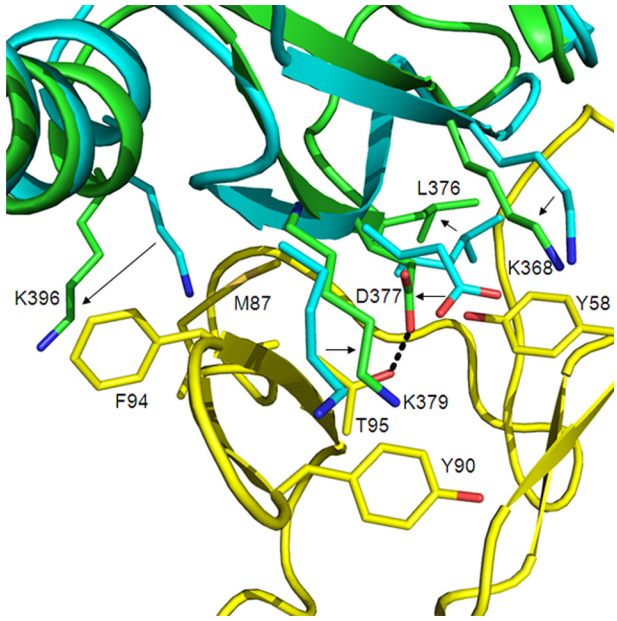

FIGURE 5. **Conformational changes to lysine residues of TolAIII on binding TA_{53-107}.** Lysine residues, Lys-368 and Lys-396, are shifted on binding the TolA box of ColA and realign with the aromatic residues Tyr-58 and Phe-94, respectively, forming stabilizing cation-π interactions. Residues Leu-376 and Asp-377 are favorably shifted to accommodate the formation of the two cation-π interactions. Asp-377 forms a hydrogen bond (*dashed line*) with Thr-96 across the binding interface of the two polypeptides. *Arrows* indicate the size and direction of the conformational shifts.

structure of TolAIII fused with g3p. Our TolAIII structure was solved by molecular replacement using the structure of TolAIII from the TA_{53-107}-TolAIII complex as a search model. This is consistent with comparisons of the root mean square distance (r.m.s.d.) of the C_α atoms of the free TolAIII x-ray structure with other TolAIII structures; the r.m.s.d. values are 2.08, 1.549, 1.673, and 0.537 when compared with PDB IDs 1LRO, 1S62, 1Tol, and 3QDR (TolAIII in complex with TA_{53-107}), respectively. Helix II runs from residues 385–370 in PDB ID 1S62 and from residues 390–370 in PDB ID 3QDP, whereas Helix III is the same in both structures and includes residues 410–413 (supplemental Fig. S4). Helix I is shorter in PDB ID 3QDP and might be a consequence of the methylation of Lys-345 (supplemental Fig. S3). However, *in silico* mutagenesis of Lys-345 to Ala did not produce any extra helicity to Helix I. β-Strands 1 and 2 in PDB ID 1S62 are linked by a short hairpin and are longer than their counterparts in PDB ID 3QDP, whereas three shorter β-strands in PDB ID 3QDP form an antiparallel β-sheet (supplemental Fig. S4). The partially ordered segment that connects helix I and β-strand 1 shows differences between the two structures with C_α atoms r.m.s.d. of 1.83 Å.

Cation-π Interactions in TA_{53-107}-TolAIII Complex—Geometrical analysis for cation-π interactions in the interface of the complex shows that three putative cation-aromatic contacts have suitable geometry. The NZ atoms of Lys-368, Lys-379, and Lys-396 of TolAIII, none of which are methylated, align above the aromatic rings of Tyr-58, Tyr-90, and Phe-94 of TA_{53-107}, respectively (Fig. 4, supplemental Table S1). The cation-π interactions were analyzed by using the CaPTURE server (44), which predicted that the three pairs of Tyr-58–Lys-368, Tyr-90–Lys-379, and Phe-94–Lys-396 were energetically significant with electrostatic energies of −3.62, −3.32, and −2.78 kcal/mol, respectively. These three cation-π interactions are located on the two sides of the β-sheet in the complex. The hydrophobic/apolar contacts mainly involve the side chains of Met-87 and Phe-94 from TA_{53-107} and Leu-375, Ile-378, Leu-392, and Lys-396 from TolAIII that form a hydrophobic patch between the β-sheet and the second α-helix.

Superposition of TolAIII in complex with the TolAIII binding region of ColA and the solution structure of TolAIII (PDB ID: 1S62) reveals some side chain rearrangements at the interface with TA_{53-107} (Fig. 5). A significant rearrangement occurs from the movement of the side chain of Lys-396 of TolAIII, which makes space for the side chain of Met-87 and positions the side chain of Lys-396 directly over the aromatic ring of Phe-94, thus forming a cation-π interaction between both residues (Fig. 5). Less dramatic rearrangements of the side chains of Lys-379 and Lys-368 result in the juxtaposition of each residue with Tyr-90 and Tyr-58, respectively, allowing the formation of two further cation-π interactions across the binding interface. Interestingly, the relocation of the side chain of Asp-377 of TolAIII toward TA_{53-107} leads to the breakage of a salt bridge between Asp-377 and Lys-368 (observed in the free TolAIII structure) and establishment of a hydrogen bond between Asp-377 and Thr-95. In addition, the side chain of Leu-376 of TolAIII moves away from the TolA binding region, liberating Tyr-58 for the cation-π interaction with Lys-368 (Figs. 4 and 5).

The significance of the three cation-π interactions on the formation of the TA_{53-107}-TolAIII complex was investigated by engineering the mutations Y58A, Y90A, and F94A in the TolA box of ColA and assessing the impact of these substitutions on both binding and biological activity. Comparison by surface plasmon resonance showed that TA_{1-107} Y90A and TA_{1-107} F94A had almost identical binding affinities with TolAIII as TA_{1-107}, whereas no interaction of TolAIII was detected with TA_{1-107} Y58A, indicating an important role for Tyr-58 in sta-

bilizing the interaction of $TA_{53–107}$ with TolAIII (supplemental Fig. S5*A*). Consistent with these binding data, Y90A and F94A had no effect on the biological activity of ColA, whereas Y58A had significantly reduced activity when compared with wild-type ColA (Fig. 3; supplemental Fig. S5*B*).

DISCUSSION

This work describes the first crystal structure of TolA in complex with a colicin translocation domain and also reveals for the first time the interaction of a Tol protein with a globular colicin domain. The interface of the complex of TolAIII with the $TA_{53–107}$ region of ColA comprises polar interactions involving residues within β-strands of each protein, further augmented by intermolecular cation-π interactions. The β-strand residues involved in contact across the interface align in an antiparallel fashion, and those from both the $TA_{53–107}$ protein (92–96) and TolA (375–380) exhibit a significant degree of surface exposure. The average relative solvent accessibilities for all side chain atoms of these residues, calculated using Naccess (68), are >64 and >46%, respectively. An exhaustive search of the PDB allowed Remaut and Waksman (57) to classify protein-protein and protein-peptide complexes involving the association of a β-strand from a ligand with a β-strand or a β-sheet in a binding partner into three distinct classes: (i) β-sheet augmentation, (ii) β-strand insertion and fold complementation, or (iii) β-strand zippering. The protein-protein interface described by the x-ray structure here would appear to represent the classical β-sheet augmentation where the interaction is mediated by a β-strand from one protein pairing to the edge of a β-sheet in the binding domain of another protein (Fig. 1).

Although methylation was essential to obtain our x-ray structures of TolAIII and the $TA_{53–107}$-TolAIII complex, we do not believe that methylation itself introduced any significant differences that affected the interpretation of the results. Our evidence for this is partly because of the observed similarity in the ^{1}H-^{15}N HSQC NMR spectra of the complex of ^{15}N-labeled $TA_{53–107}$ bound to unlabeled TolAIII with and without *N*-methylation (supplemental Fig. S6) and the fact that different patterns of methylation were observed in both free and complexed TolAIII. Although differences do exist between the structures of TolAIII determined by x-ray (herein) and NMR methods (25), they are small, and the residues predicted to be important in the interaction of TolAIII with $TA_{53–107}$ by NMR (27) are identical to those residues shown to be involved in the x-ray structure of the $TA_{53–107}$-TolAIII complex (Fig. 2). The x-ray data of TolAIII alone or in complex with $TA_{53–107}$ are also identical apart from the conformational changes exerted by interacting residues across the interface of the two proteins (Fig. 5).

The contribution of individual residues of both TolAIII and $TA_{53–107}$ to the binding interface of the $TA_{53–107}$-TolAIII complex was determined by alanine-scanning mutagenesis. No mutation of a single residue at the interface in either $TA_{53–107}$ or TolAIII prevented the interaction with the partner protein (Fig. 3; Table 2). This is very different from the interaction observed for the TolB box of ColA and TolB whereby mutations to individual residues that contribute intramolecular bonds to the fold of the TolB box on binding TolB abolish the interaction with TolB (24, 45). As the hydrogen bonds between residues Phe-94 and Thr-95 of $TA_{53–107}$ and Leu-375, Leu-376, and Ile-378 of TolAIII occur from backbone atoms, this mutagenesis result is perhaps unsurprising (Fig. 2). However, the hydrogen bonds between residues Arg-92 and Arg-96 of $TA_{53–107}$ are from side chain atoms specific to each arginine residue, which might be expected to be essential for the formation of the interaction between the two polypeptides. However, no significant loss of activity of ColA was observed when the mutations R92A and R96A were engineered into ColA simultaneously (Fig. 3).

This is the first reported example of a colicin-ligand interaction in which cation-π interactions contribute to the interacting complex. The importance of each cation-π interaction was initially assessed from the x-ray structure (Fig. 4; PDB ID: 3QDR). Tyr-58 –Lys-368 has much closer, better coordinated dipoles than the other two paired residues and would perhaps be expected to contribute stronger electrostatic interactions. Mutagenesis of all three aromatic residues of the TolA binding region that are involved in cation-π interactions, and analysis of the interaction of the mutated polypeptides with TolA by biological activity assays and surface plasmon resonance, confirmed that Tyr-58 was essential for complex formation, whereas Tyr-90 and Phe-94 were not essential (supplemental Fig. S5, Fig. 3). Pommier *et al.* (15) had previously identified Tyr-58 and Tyr-90 within two putative TolA binding regions of ColA. Cation-π interactions have been shown to be vital in the translocation of lethal factor through the protective antigen channel of the anthrax toxin by establishing a protein-protein tether that encourages unidirectional movement of the toxin into the cytosol of endocytosed cells by a Brownian ratchet motion (58).

ColA is unique in colicin biology in possessing different binding epitopes for two Tol proteins. A detailed model for the recruitment of TolB by the TolB box of ColE9 has been presented (59, 60). Such models have to be extended to explain the translocation of ColA to accommodate the additional interaction of the TolA binding site with TolA. It has been proposed that the translocation domain of ColA interacts firstly with TolB in the periplasm, via a low affinity interaction of its TolB box, and then with TolA via a higher affinity interaction with its TolA binding site (24). The structural and mutagenesis information in this study provides more detail of the latter interaction.

Filamentous phages infect *E. coli* in a two-step process that involves the interaction of two N-terminal domains of the g3p protein of phage fd (N2 and N1) that bind to cell pili and TolAIII, respectively, in a sequential manner (26). In the fully folded form of g3p, the N1 and N2 domains are tightly associated and without disassociation of both domains by the binding of N2 to the cell pilus, N1 is unable to interact with TolAIII, and the virus is noninfective. However, the structure of the $TA_{53–107}$-TolAIII complex reveals that the TolA binding region of ColA binds to a different region of TolAIII than that to which g3p binds (26), with no single residue of TolAIII being involved in binding to both proteins (Figs. 6 and 7).

There is currently no published evidence to suggest that the TolA binding site and the TolB box of ColA interact with each

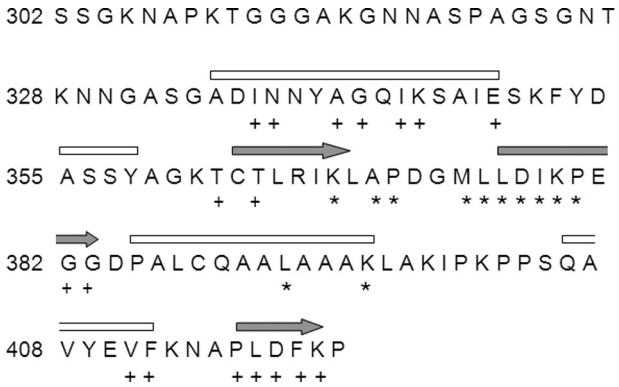

FIGURE 6. **Primary sequence of TolAIII.** Helical (*white boxes*) and β-sheet (*gray arrow*) regions are shown above the primary sequence of TolAIII. Residue numbers in TolA are shown to the *left*. Residues interacting with the TolA binding region of ColA (*) are very different from residues that interact with g3p (+). A His_6 tag with the sequence MAKHHHHHHM was engineered at the N terminus of TolAIII to promote efficient purification and avoid the important C terminus of TolAIII.

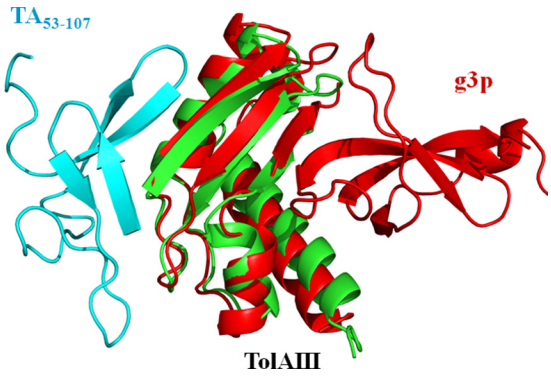

FIGURE 7. **Comparison of structures of TolAIII in complex with TA_{53-107} and g3p.** Structures of TA_{53-107} (*blue*) in complex with TolAIII (*green*) and g3p (*red*) in complex with TolAIII (*red*) were overlaid using the PyMOL program (67), showing that both ligands form β-strand addition pairs to opposing β-sheets of TolAIII. The interactions of both do not cause any major conformational changes to the tertiary structure of TolAIII.

other in a similar way to the N1 and N2 domains of g3p. However, we have preliminary NMR data showing that the chemical shifts of a mixture of the TA_{1-52} and TA_{53-107} peptides were slightly different for some residues of TA_{53-107} when compared with those of TA_{53-107} on its own.[7] NMR data have shown that a truncated polypeptide expressing both the TolA binding region and the TolB box of ColA causes an unfolding of TolAIII *in vitro*, which is not apparent when the TolA binding region and TolB boxes are physically separated and added to TolAIII concurrently (27). If TolA binds TolB and ColA at different binding interfaces in the TA_{1-107}-TolA-TolB trimeric complex, then it is possible that an unoccupied TolB box of ColA could interfere and cause localized unfolding of TolAIII in the TA_{1-107}-TolAIII complex as unfolding of TolAIII is not observed on binding of the translocation domain of ColN, which does not possess a TolB box (27). Interestingly, the TolA binding region of ColN forms intramolecular contacts with globular regions of the protein as a means of enhanced protection against proteolytic cleavage rather than domain inactivation, as seen with phage fd (29).

[7] G. M. Moore, unpublished data.

The binding interface of the TolA binding region of ColA presented here shows a unique fold that binds on the opposite side of TolAIII to a conserved hydrophobic cavity that forms the interface with the g3p protein (26), which has been reported as influential for conformational changes of TolAIII important for interacting with different binding partners in *E. coli* (25) and *Pseudomonas aeruginosa* (61). Recent NMR data on the interaction of TolAIII with ColN have also predicted a similar binding interface to that of g3p-TolAIII, but the precise details of the interaction of ColN with the hydrophobic cavity of TolAIII have not yet been elucidated.[7] It has recently been demonstrated that TolA interacts with TolB as a prerequisite to the translocation of the enzymatic colicin, ColE9 (60). The interaction is believed to involve the extreme N terminus of TolB, but the interacting region of TolA is currently unknown. However, the similarity of the ^{1}H-^{15}N HSQC NMR spectrum of TolAIII in the B^{1-13}-TolAIII complex (supplemental Fig. S7) with that of ColN-TolAIII (29) suggests that B^{1-13} binds TolAIII in a similar manner to ColN and g3p. TolA has also been predicted to interact with ColE1 differently than other group A colicins (62) and with YbgF via TolAII (63), and therefore, TolA exhibits the properties of a promiscuous hub protein that interacts with both intrinsic and extrinsic proteins through several different interaction sites (64). Apart from interacting networks involved in peptidoglycan synthesis and cell envelope biogenesis (65), the only other well characterized set of interacting periplasmic proteins consists of those linked by the hub protein NDsbD that are involved in disulfide isomerization (66). Several colicins and bacteriophages have taken advantage of the promiscuity afforded them by TolA for unimpeded entry into an *E. coli* cell. Elucidation of structural data on the interaction of TolA with TolB will not only extend our understanding of the pivotal role of TolA in cell function and homeostasis of Gram-negative bacteria, but will enhance opportunities of using TolA as a drug target for antimicrobial treatments.

Acknowledgments—We thank Sitthanan Thanintranon for construction of single TolAIII mutants. We are grateful to the European Synchrotron Radiation Facility at Grenoble, France for data collection.

REFERENCES

1. Sturgis, J. (2001) Organization and evolution of the tol-pal gene cluster. *J. Mol. Microbiol. Biotechnol.* **3,** 113–122
2. Cascales, E., Lloubès, R., and Sturgis, J. N. (2001) The TolQ-TolR proteins energize TolA and share homologies with the flagellar motor proteins MotA-MotB. *Mol. Microbiol.* **42,** 795–807
3. Goemaere, E. L., Cascales, E., and Lloubès, R. (2007) Mutational analyses define helix organization and key residues of a bacterial membrane energy-transducing complex. *J. Mol. Biol.* **366,** 1424–1436
4. Gerding, M. A., Ogata, Y., Pecora, N. D., Niki, H., and de Boer, P. A. (2007) The trans-envelope Tol-Pal complex is part of the cell division machinery and required for proper outer-membrane invagination during cell constriction in *E. coli*. *Mol. Microbiol.* **63,** 1008–1025
5. Germon, P., Ray, M. C., Vianney, A., and Lazzaroni, J. C. (2001) Energy-dependent conformational change in the TolA protein of *Escherichia coli* involves its N-terminal domain, TolQ, and TolR. *J. Bacteriol.* **183,** 4110–4114
6. Dubuisson, J. F., Vianney, A., and Lazzaroni, J. C. (2002) Mutational analysis of the TolA C-terminal domain of *Escherichia coli* and genetic evidence for an interaction between TolA and TolB. *J. Bacteriol.* **184,**

4620–4625
7. Walburger, A., Lazdunski, C., and Corda, Y. (2002) The Tol/Pal system function requires an interaction between the C-terminal domain of TolA and the N-terminal domain of TolB. *Mol. Microbiol.* **44,** 695–708
8. Cascales, E., Gavioli, M., Sturgis, J. N., and Lloubès, R. (2000) Proton motive force drives the interaction of the inner membrane TolA and outer membrane Pal proteins in *Escherichia coli*. *Mol. Microbiol.* **38,** 904–915
9. Lloubès, R., Cascales, E., Walburger, A., Bouveret, E., Lazdunski, C., Bernadac, A., and Journet, L. (2001) The Tol-Pal proteins of the *Escherichia coli* cell envelope: an energized system required for outer membrane integrity? *Res. Microbiol.* **152,** 523–529
10. Cascales, E., Bernadac, A., Gavioli, M., Lazzaroni, J. C., and Lloubès, R. (2002) Pal lipoprotein of *Escherichia coli* plays a major role in outer membrane integrity. *J. Bacteriol.* **184,** 754–759
11. Bouveret, E., Derouiche, R., Rigal, A., Lloubès, R., Lazdunski, C., and Bénédetti, H. (1995) Peptidoglycan-associated lipoprotein-TolB interaction: a possible key to explaining the formation of contact sites between the inner and outer membranes of *Escherichia coli*. *J. Biol. Chem.* **270,** 11071–11077
12. Baty, D., Lakey, J., Pattus, F., and Lazdunski, C. (1990) A 136-amino-acid-residue COOH-terminal fragment of colicin A is endowed with ionophoric activity. *Eur. J. Biochem.* **189,** 409–413
13. Bouveret, E., Rigal, A., Lazdunski, C., and Bénédetti, H. (1998) Distinct regions of the colicin A translocation domain are involved in the interaction with TolA and TolB proteins upon import into *Escherichia coli*. *Mol. Microbiol.* **27,** 143–157
14. Journet, L., Bouveret, E., Rigal, A., Lloubès, R., Lazdunski, C., and Bénédetti, H. (2001) Import of colicins across the outer membrane of *Escherichia coli* involves multiple protein interactions in the periplasm. *Mol. Microbiol.* **42,** 331–344
15. Pommier, S., Gavioli, M., Cascales, E., and Lloubès, R. (2005) Tol-dependent macromolecule import through the *Escherichia coli* cell envelope requires the presence of an exposed TolA binding motif. *J. Bacteriol.* **187,** 7526–7534
16. Raggett, E. M., Bainbridge, G., Evans, L. J., Cooper, A., and Lakey, J. H. (1998) Discovery of critical Tol A-binding residues in the bactericidal toxin colicin N: a biophysical approach. *Mol. Microbiol.* **28,** 1335–1343
17. Webster, R. E. (1991) The *tol* gene products and the import of macromolecules into *Escherichia coli*. *Mol. Microbiol.* **5,** 1005–1011
18. Riechmann, L., and Holliger, P. (1997) The C-terminal domain of TolA is the coreceptor for filamentous phage infection of *E. coli*. *Cell* **90,** 351–360
19. Bonsor, D. A., Meenan, N. A., and Kleanthous, C. (2008) Colicins exploit native disorder to gain cell entry: a hitchhiker's guide to translocation. *Biochem. Soc. Trans.* **36,** 1409–1413
20. Kleanthous, C. (2010) Swimming against the tide: progress and challenges in our understanding of colicin translocation. *Nat. Rev. Microbiol.* **8,** 843–848
21. Housden, N. G., Wojdyla, J. A., Korczynska, J., Grishkovskaya, I., Kirkpatrick, N., Brzozowski, A. M., and Kleanthous, C. (2010) Directed epitope delivery across the *Escherichia coli* outer membrane through the porin OmpF. *Proc. Natl. Acad. Sci. U.S.A.* **107,** 21412–21417
22. Bonsor, D. A., Grishkovskaya, I., Dodson, E. J., and Kleanthous, C. (2007) Molecular mimicry enables competitive recruitment by a natively disordered protein. *J. Am. Chem. Soc.* **129,** 4800–4807
23. Loftus, S. R., Walker, D., Maté, M. J., Bonsor, D. A., James, R., Moore, G. R., and Kleanthous, C. (2006) Competitive recruitment of the periplasmic translocation portal TolB by a natively disordered domain of colicin E9. *Proc. Natl. Acad. Sci. U.S.A.* **103,** 12353–12358
24. Zhang, Y., Li, C., Vankemmelbeke, M. N., Bardelang, P., Paoli, M., Penfold, C. N., and James, R. (2010) The crystal structure of the TolB box of colicin A in complex with TolB reveals important differences in the recruitment of the common TolB translocation portal used by group A colicins. *Mol. Microbiol.* **75,** 623–636
25. Deprez, C., Lloubès, R., Gavioli, M., Marion, D., Guerlesquin, F., and Blanchard, L. (2005) Solution structure of the *E. coli* TolA C-terminal domain reveals conformational changes upon binding to the phage g3p N-terminal domain. *J. Mol. Biol.* **346,** 1047–1057
26. Lubkowski, J., Hennecke, F., Plückthun, A., and Wlodawer, A. (1999) Filamentous phage infection: crystal structure of g3p in complex with its coreceptor, the C-terminal domain of TolA. *Structure* **7,** 711–722
27. Hecht, O., Zhang, Y., Li, C., Penfold, C. N., James, R., and Moore, G. R. (2010) Characterization of the interaction of colicin A with its co-receptor TolA. *FEBS Lett.* **584,** 2249–2252
28. Delaglio, F., Grzesiek, S., Vuister, G. W., Zhu, G., Pfeifer, J., and Bax, A. (1995) NMRPipe: a multidimensional spectral processing system based on UNIX pipes. *J. Biomol. NMR.* **6**, 277–293
29. Hecht, O., Ridley, H., Boetzel, R., Lewin, A., Cull, N., Chalton, D. A., Lakey, J. H., and Moore, G. R. (2008) Self-recognition by an intrinsically disordered protein. *FEBS Lett.* **582,** 2673–2677
30. Walter, T. S., Meier, C., Assenberg, R., Au, K. F., Ren, J., Verma, A., Nettleship, J. E., Owens, R. J., Stuart, D. I., and Grimes, J. M. (2006) Lysine methylation as a routine rescue strategy for protein crystallization. *Structure* **14,** 1617–1622
31. Rayment, I. (1997) Reductive alkylation of lysine residues to alter crystallization properties of proteins. *Methods Enzymol.* **276,** 171–179
32. Leslie, A. G. (1992) *Joint CCP4 and ESF-EACMB Newsletter on Protein Crystallography,* Vol. 26, Collaborative Computational Project Number 4 in Protein Crystallography, Oxon, UK
33. Evans, P. (2006) Scaling and assessment of data quality. *Acta Crystallogr. D Biol. Crystallogr.* **62,** 72–82
34. Evans, P. (1997) *CCP4 Newsletter on Protein Crystallography,* Vol. 33, pp. 22–24, Collaborative Computational Project Number 4 in Protein Crystallography, Oxon, UK
35. Collaborative Computational Project, Number 4 (1994) The CCP4 suite: programs for protein crystallography. *Acta Crystallogr. D Biol. Crystallogr.* **50,** 760–763
36. McCoy, A. J., Grosse-Kunstleve, R. W., Adams, P. D., Winn, M. D., Storoni, L. C., and Read, R. J. (2007) Phaser crystallographic software. *J. Appl. Crystallogr.* **40,** 658–674
37. Terwilliger, T. C., and Berendzen, J. (1999) Automated MAD and MIR structure solution. *Acta Crystallogr. D Biol. Crystallogr.* **55,** 849–861
38. Cowtan, K. (1999) Error estimation and bias correction in phase-improvement calculations. *Acta Crystallogr. D Biol. Crystallogr.* **55,** 1555–1567
39. Cowtan, K. (2006) The Buccaneer software for automated model building. 1. Tracing protein chains. *Acta Crystallogr. D Biol. Crystallogr.* **62,** 1002–1011
40. Emsley, P., and Cowtan, K. (2004) Coot: model-building tools for molecular graphics. *Acta Crystallogr. D Biol. Crystallogr.* **60,** 2126–2132
41. Murshudov, G. N., Vagin, A. A., and Dodson, E. J. (1997) Refinement of macromolecular structures by the maximum-likelihood method. *Acta Crystallogr. D Biol. Crystallogr.* **53,** 240–255
42. Painter, J., and Merritt, E. A. (2006) TLSMD web server for the generation of multi-group TLS models. *J. Appl. Crystallogr.* **39,** 109–111
43. Lee, B., and Richards, F. M. (1971) The interpretation of protein structures: estimation of static accessibility. *J. Mol. Biol.* **55,** 379–400
44. Gallivan, J. P., and Dougherty, D. A. (1999) Cation-π interactions in structural biology. *Proc. Natl. Acad. Sci. U.S.A.* **96,** 9459–9464
45. Hands, S. L., Holland, L. E., Vankemmelbeke, M., Fraser, L., Macdonald, C. J., Moore, G. R., James, R., and Penfold, C. N. (2005) Interactions of TolB with the translocation domain of colicin E9 require an extended TolB box. *J. Bacteriol.* **187,** 6733–6741
46. Yang, Z. R., Thomson, R., McNeil, P., and Esnouf, R. M. (2005) RONN: the bio-basis function neural network technique applied to the detection of natively disordered regions in proteins. *Bioinformatics* **21,** 3369–3376
47. Macdonald, C. J., Tozawa, K., Collins, E. S., Penfold, C. N., James, R., Kleanthous, C., Clayden, N. J., and Moore, G. R. (2004) Characterization of a mobile protein-binding epitope in the translocation domain of colicin E9. *J. Biomol. NMR* **30,** 81–96
48. Tozawa, K., Macdonald, C. J., Penfold, C. N., James, R., Kleanthous, C., Clayden, N. J., and Moore, G. R. (2005) Clusters in an intrinsically disordered protein create a protein-binding site: the TolB-binding region of colicin E9. *Biochemistry* **44,** 11496–11507
49. Collins, E. S., Whittaker, S. B., Tozawa, K., MacDonald, C., Boetzel, R., Penfold, C. N., Reilly, A., Clayden, N. J., Osborne, M. J., Hemmings, A. M., Kleanthous, C., James, R., and Moore, G. R. (2002) Structural dynamics of the membrane translocation domain of colicin E9 and its interaction with

TolB. *J. Mol. Biol.* **318,** 787–804
50. Deprez, C., Blanchard, L., Guerlesquin, F., Gavioli, M., Simorre, J. P., Lazdunski, C., Marion, D., and Lloubès, R. (2002) Macromolecular import into *Escherichia coli*: the TolA C-terminal domain changes conformation when interacting with the colicin A toxin. *Biochemistry* **41,** 2589–2598
51. Goldschmidt, L., Cooper, D. R., Derewenda, Z. S., and Eisenberg, D. (2007) Toward rational protein crystallization: a Web server for the design of crystallizable protein variants. *Protein Sci.* **16,** 1569–1576
52. Lo Conte, L., Chothia, C., and Janin, J. (1999) The atomic structure of protein-protein recognition sites. *J. Mol. Biol.* **285,** 2177–2198
53. Bahadur, R. P., and Zacharias, M. (2008) The interface of protein-protein complexes: analysis of contacts and prediction of interactions. *Cell. Mol. Life Sci.* **65,** 1059–1072
54. Lawrence, M. C., and Colman, P. M. (1993) Shape complementarity at protein/protein interfaces. *J. Mol. Biol.* **234,** 946–950
55. Gokce, I., Raggett, E. M., Hong, Q., Virden, R., Cooper, A., and Lakey, J. H. (2000) The TolA-recognition site of colicin N: ITC, SPR, and stopped-flow fluorescence define a crucial 27-residue segment. *J. Mol. Biol.* **304,** 621–632
56. Bernadac, A., Gavioli, M., Lazzaroni, J. C., Raina, S., and Lloubès, R. (1998) *Escherichia coli tol-pal* mutants form outer membrane vesicles. *J. Bacteriol.* **180,** 4872–4878
57. Remaut, H., and Waksman, G. (2006) Protein-protein interaction through β-strand addition. *Trends Biochem. Sci.* **31,** 436–444
58. Krantz, B. A., Melnyk, R. A., Zhang, S., Juris, S. J., Lacy, D. B., Wu, Z., Finkelstein, A., and Collier, R. J. (2005) A phenylalanine clamp catalyzes protein translocation through the anthrax toxin pore. *Science* **309,** 777–781
59. Papadakos, G., Housden, N. G., Lilly, K. J., Kaminska, R., and Kleanthous, C. (2012) Kinetic basis for the competitive recruitment of TolB by the intrinsically disordered translocation domain of colicin E9. *J. Mol. Biol.* **418,** 269–280
60. Bonsor, D. A., Hecht, O., Vankemmelbeke, M., Sharma, A., Krachler, A. M., Housden, N. G., Lilly, K. J., James, R., Moore, G. R., and Kleanthous, C. (2009) Allosteric β-propeller signaling in TolB and its manipulation by translocating colicins. *EMBO J.* **28,** 2846–2857
61. Witty, M., Sanz, C., Shah, A., Grossmann, J. G., Mizuguchi, K., Perham, R. N., and Luisi, B. (2002) Structure of the periplasmic domain of *Pseudomonas aeruginosa* TolA: evidence for an evolutionary relationship with the TonB transporter protein. *EMBO J.* **21,** 4207–4218
62. Schendel, S. L., Click, E. M., Webster, R. E., and Cramer, W. A. (1997) The TolA protein interacts with colicin E1 differently than with other group A colicins. *J. Bacteriol.* **179,** 3683–3690
63. Krachler, A. M., Sharma, A., Cauldwell, A., Papadakos, G., and Kleanthous, C. (2010) TolA modulates the oligomeric status of YbgF in the bacterial periplasm. *J. Mol. Biol.* **403,** 270–285
64. Patil, A., Kinoshita, K., and Nakamura, H. (2010) Hub promiscuity in protein-protein interaction networks. *Int. J. Mol. Sci.* **11,** 1930–1943
65. Hu, P., Janga, S. C., Babu, M., Díaz-Mejía, J. J., Butland, G., Yang, W., Pogoutse, O., Guo, X., Phanse, S., Wong, P., Chandran, S., Christopoulos, C., Nazarians-Armavil, A., Nasseri, N. K., Musso, G., Ali, M., Nazemof, N., Eroukova, V., Golshani, A., Paccanaro, A., Greenblatt, J. F., Moreno-Hagelsieb, G., and Emili, A. (2009) Global functional atlas of *Escherichia coli* encompassing previously uncharacterized proteins. *PLoS biol* **7,** e96
66. Stirnimann, C. U., Grütter, M. G., Glockshuber, R., and Capitani, G. (2006) nDsbD: a redox interaction hub in the *Escherichia coli* periplasm. *Cell. Mol. Life Sci.* **63,** 1642–1648
67. DeLano, W. L. (2010) *The PyMOL Molecular Graphics System*, version 1.3r1, Schrödinger, LLC, New York
68. Hubbard, S., and Thornton, J. (1996) Naccess, University of Manchester, Manchester, U.K.